Anionic Amphiphilic Calixarenes for Peptide Assembly and Delivery

Roman Rodik, Sergiy Cherenok, Viktoriia Postupalenko, Sule Oncul, Vladyslava Brusianska, Petro Borysko, Vitaly Kalchenko, Yves Mely, Andrey Klymchenko

Anionic Amphiphilic Calixarenes for Peptide Assembly and Delivery

Roman V. Rodik,[a,*] Sergiy O. Cherenok,[a] Viktoriia Y. Postupalenko,[b] Sule Oncul,[b,c] Vladyslava Brusianska,[d] Petro Borysko,[d] Vitaly I. Kalchenko,[a] Yves Mely,[b] Andrey S. Klymchenko.[b,*]

[a] Institute of Organic Chemistry, National Academy of Science of Ukraine, 02660, Kyiv, Ukraine.

[b] Laboratoire de Bioimagerie et Pathologies, UMR 7021 CNRS, Université de Strasbourg, Faculté de Pharmacie, 74, Route du Rhin, 67401 ILLKIRCH Cedex, France.

[c] İstanbul Medeniyet Üniversitesi, Istanbul, Turkey

[d] Enamine Ltd, Chervonotkatska 78, 02094 Kyiv, Ukraine

*Corresponding authors: dmso@ukr.net; andrey.klymchenko@unistra.fr

Abstract

Shape-persistent macrocycles enable superior control on molecular self-assembly, allowing the preparation of well-defined nanostructures with new functions. Here, we report on anionic amphiphilic calixarenes of conic shape and their self-assembly behavior in aqueous media for application in intracellular delivery of peptides. Newly synthesized calixarenes bearing four phosphonate groups and two or four long alkyl chains were found to form micelles of ~10 nm diameter, in contrast to an analogue with short alkyl chains. These amphiphilic calixarenes are able to complex model (oligo-lysine) and biologically relevant (HIV-1 nucleocapsid peptide) cationic peptides into small nanoparticles (20-40 nm). By contrast, a control anionic calixarene with short alkyl chains fails to form small nanoparticles with peptides, highlighting the importance of micellar assembly of amphiphilic calixarenes for peptide complexation. Cellular studies reveal that anionic amphiphilic calixarenes exhibit low cytotoxicity and enable internalization of fluorescently labelled peptides into live cells. These findings suggest anionic amphiphilic macrocycles as promising building blocks for the preparation of peptide delivery vehicles.

Keywords: shape-persistent surfactants, anionic amphiphilic macrocycles, self-assembly, micelles, peptide-surfactant interactions, peptide nanoparticles, peptide delivery, cell internalization, fluorescence spectroscopy, fluorescence microscopy.

Introduction

Use of peptides as drugs [1-3] raises questions about their effective delivery [4-6]. A number of methodologies for peptide/protein delivery have been developed, including those using cell-penetrating peptides [7-9], mesoporous silica nanoparticles [10], lipid nanocarriers [5, 11, 12], and polymers [4, 13, 14] and different supramolecular approaches [15]. Among existing delivery vehicles, synthetic macrocycles emerged as promising tools [16-19], because their shape persistent architecture ensures the formation of well-defined assemblies [18, 20-22]. Among these macrocycles, calixarenes [23-25], resorcinarene [22, 26], pillar[n]arenes [27-29] and cucurbituril [30, 31] are particularly efficient as gene delivery vehicles. Cationic amphiphilic macrocycles have notably been shown to compact polyanionic nucleic acids into small virus-sized nanoparticles for their intracellular delivery [23, 32-34]. Calixarenes are of particular interest because these synthetically available macrocyclic molecules have well defined conical shape, which allows fabrication of a large variety of functional molecules, ranging from optical sensors and smart materials [25, 35] to functional supramolecular nanostructures [20, 36, 37] and nanocarriers of drugs and nucleic acids [16, 38-41]. In particular, cationic amphiphilic calixarenes, such as CX8 (Scheme 1), were shown to form micelles of well-defined small size (5-6 nm) [34], which subsequently through their strongly cationic surface form stable and small-size complexes with DNA biomolecule. Capacity of cationic calixarenes to assemble anionic DNA biomolecules into small nanoparticles (NPs) resulted in their applications for gene delivery [23, 32, 33, 41, 42]. Similar hierarchical assembly has been noticed for glycosylated resorcinarene, which also forms through an intermediate micellar structure [22, 26]. Therefore, we hypothesized that to form stable and small-sized complexes with cationic peptides, one should design amphiphilic anionic macrocycles prone to micellar assembly. These complexes could then be used as vehicles for the delivery of peptides into the cells. However, so far, macrocyclic compounds have not been explored for complexation and intracellular delivery of peptides. One report showed a possibility to deliver peptide nucleic acids (PNAs), although this approach used cationic tetraargininocalix[4]arene [43], similar to those used for delivery of nucleic acids [33].

In the present work, we aimed to develop first prototypes of calixarene-based nanocarriers for peptides and study their interactions with cells. Several anionic amphiphilic calixarenes were synthesized and then their self-assembly behavior and complexation with cationic peptides were characterized. We found that some of them form micellar structures capable to complex cationic peptides into small nanoparticles. The anionic calixarenes showed low cytotoxicity and enabled internalization of a model peptide inside the cells. The obtained results suggest that anionic amphiphilic macrocycles are promising delivery vectors of cationic peptides.

Results and discussion

Design and synthesis

To complex cationic peptides, one should design negatively charged calixarenes. Phosphonates were chosen as negatively charged groups. Three different anionic calixarenes were designed, CAX8, C780, and C781, with varied positioning of four phosphonate groups and different alkyl chain lengths (Scheme 1). Among them, tetraphosphonic acid calixarenes CAX8 and C780 bear four negative charges and hydrophobic alkyl chains. The tetraanionic calixarene C780 was obtained similarly to previously reported C781.[44] First, dicarboxylic acid dichlorides **2a** and **2b** were obtained from the corresponding diacid **1a** and **1b** using thionyl chloride. They were then reacted with tris-trimethylsilylphosphite ($P(OSiMe_3)_3$) followed by methanolysis, yielding target compounds C780 and C781, respectively. CAX8 is a direct analogue of cationic CX8 [23], but bearing negative charges. In the first step of CAX8 synthesis, tetraoctyl-tetrachloromethyl calixarene (**3**) was phosphorylated with tris-trimethylsilylphosphite to yield intermediate calixarene tetraphosphonate (Scheme 1). The latter calixarene was isolated as a crude product and then treated with an excess of methanol. CAX8 was obtained after evaporation of the liquid phase.

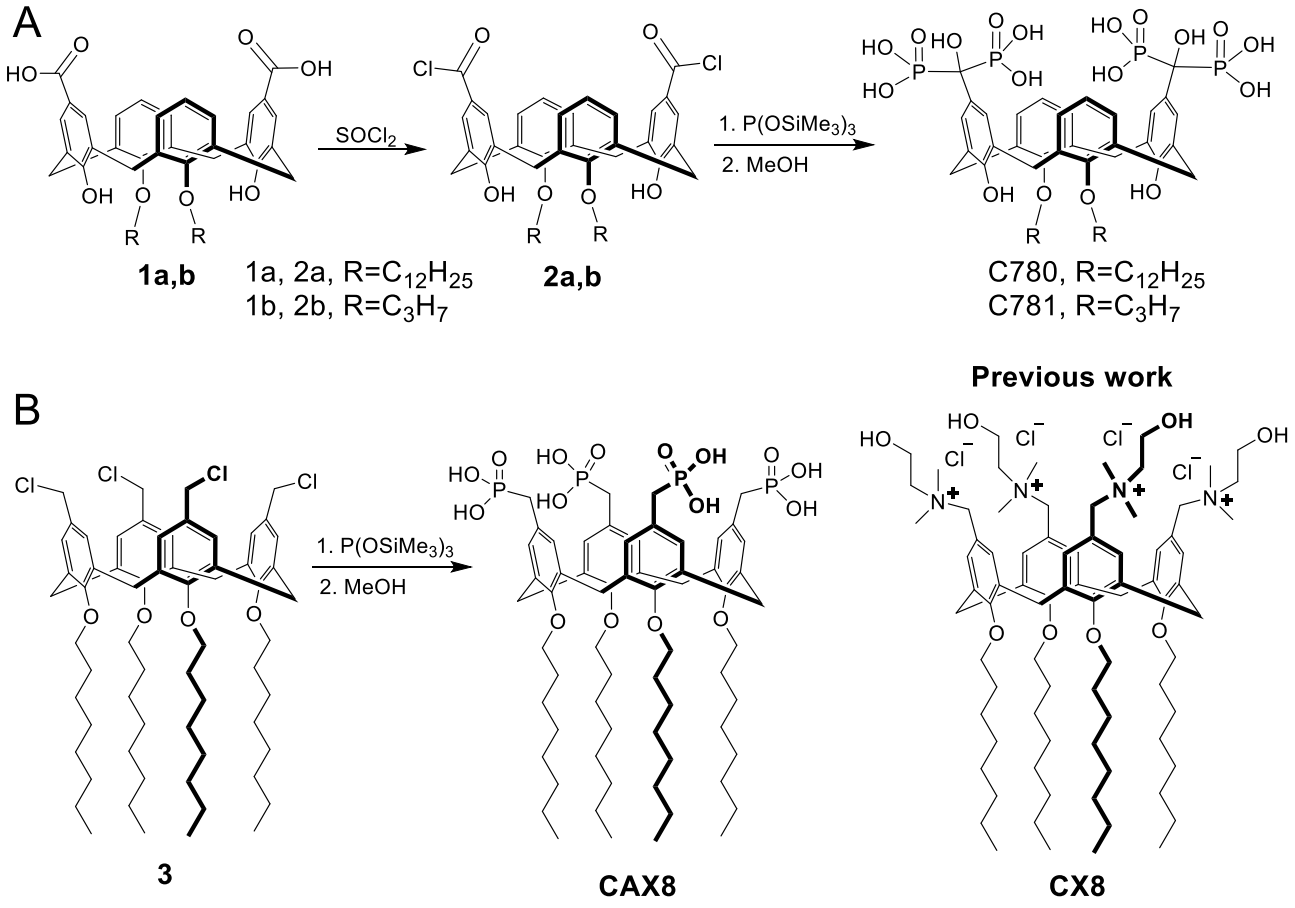

Scheme 1. Schemes of synthesis of C780, C781 (A) and CAX8 (B) and structure of CX8.

The amphiphilic nature of CAX8 is clear from its structure, but in contrast to its tetracationic analogue CX8 (Scheme 1), its solubility in water was limited. Therefore, we first prepared its stock solution in DMSO at 10 mM. The latter solution was diluted in water or buffer to different concentrations, and we found that above 200 µM concentration (at 400 µM), CAX8 showed precipitation. Moreover, when 0.1 M NaOH solution was used to dilute the CAX8 stock solution in DMSO, the highest concentration achieved was 400 µM, while at 600 µM the compound precipitated. This comparable solubility in water and 0.1 M NaOH indicates that CAX8 is probably ionized in neutral pH and does not require high pH for dissolution.

1,3-di-methylenebisphosphonic acid calixarene C780 with two dodecyl chains connected to distal rings of calixarene and four anionic groups at the upper rim is also expected to be amphiphilic. However, solubility in water was also poor and required preparation of a DMSO stock solution (up to 8 mM). The highest concentrations of C780 without precipitation were 200 µM in water or buffer and 400 µM in 0.1 M NaOH solution, which is the same as for CAX8. Nevertheless, the geometry of C780 is expected to be slightly different from that of CAX8. C780 has an elliptical frustum cone shape according to the calculation of its optimal conformation in vacuum by the PM3 semi-empirical method (Fig. S1), while the more symmetrical CAX8 has a regular frustum cone shape. Moreover, the volume of the lipophilic groups of C780 is smaller than that of CAX8. Therefore, the amphiphilic and self-assembling properties of C780 (and C781) are expected to be different from those of CAX8.

Investigation of water solutions of anionic calixarenes.

The formation of micelles or micelle-like aggregates by anionic calixarenes can be investigated by using the fluorescent environment-sensitive pyrene probe [23]. To this end, the fluorescence intensity ratio of the third and the first peaks of pyrene I3/I1 (at 384 and 373 nm, respectively) was analyzed as a function of the amphiphile concentration. Both CAX8 and C780 showed sigmoid curves with the rapid growth of the I3/I1 ratio at the micromolar range followed by saturation above 0.1 mM (Figure 1, S2 and S3). In contrast, no significant changes in the pyrene spectra were observed with C781. Thus, the pyrene probe suggested self-assembly of CAX8 and C780 in solutions, in contrast to C781. Strong hydrophobic interactions of alkyl chains probably drive the formation of micelles in the case of CAX8 and C780, which cannot be realized for C781 bearing short alkyl chains.

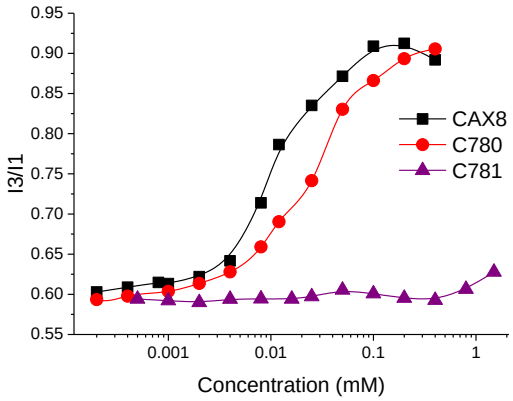

Figure 1. Fluorescence intensity ratio I3/I1 of pyrene as a function of the concentration of calixarenes in 20 mM Tris buffer, at pH 7.4.

Analysis of these curves using manual and sigmoidal fit approaches (Table S1) allowed estimation of critical micellar concentration (CMC, Table 1). Unexpectedly, CAX8 in neat water displayed a ~10-fold lower CMC value compared to its cationic analogue CX8 [23]. Probably, the reason is the lower effective charge of phosphonate and its capacity to form intermolecular H-bonds compared to the ammonium groups, which decreases repulsion of head groups within the micelles. The weak effects of salts on CMC of CAX8 and C780 (Table 1), in contrast to CX8 [23], confirms that additional forces, including H-bonding, can control micelle formation. On the other hand, C781 CMC was not detectable because its two propyl chains were not sufficiently lipophilic.

Table. 1 CMC and hydrodynamic diameter values for all calixarenes in aqueous media.

	CAX8	C780	C781
CMC, water (μM)	3.0±0.2	5.4±3.7	Non
Diameter, water[a] (nm)	18±0.5	7.7±0.1	370±16
CMC, buffer[b] (μM)	3.0±0.4	5.8±1.0	Non

[a] Hydrodynamic diameter measured by DLS for anionic calixarenes (1.5×10^{-4} M) in water; [b] 20 mM Tris buffer, pH 7.4. CMC value is an average of manual and sigmoidal fit approaches; error is standard deviation. Diameter is a mean of 3 measurements; error is standard deviation.

Dynamic light scattering (DLS) measurements suggested that the micelle size was 18 and 7.7 nm for CAX8 and C780, respectively (Table 1, Figures S4-S6). Normally, the diameter of calixarene micelles should be approximately twice the length of a calixarene along its main axis (Scheme 2A) [23]. According to calculations, calixarene C780 adopts a *pinched cone* conformation, having a shape of an

elliptical frustum cone (Figure S1). The main characteristics are elliptical base diameters 0.86 nm and 1.35 nm, section diameter 0.45 nm, and length 2.26 nm. Therefore, the full length of the predicted cone is 3.85 nm and thus, the micelle diameter should be ≥ 7.7 nm, in full line with the average diameter of 7.7 nm measured by DLS. On the other hand, calixarene CAX8 adopts *regular cone* conformation with the shape of a frustum cone (Figure S1). The main characteristics are base diameter 1.02 nm, section diameter 0.51 nm, and length 1.76 nm. This frustum cone has a sharper angle than CX8 and the full length of the predicted cone is 3.5 nm which corresponds to a micelle diameter of ≥ 7 nm. The average diameter of 18 nm measured by DLS for CAX8 particles is 2-3 times larger than the calculated one. We can consider two possible explanations. First, the presence of four alkyl chains (CAX8) instead of two (C780) makes the lipophilic part of the amphiphile too bulky inside the hydrophobic part, which can be less favorable for micelle formation, allowing other types of assemblies. Moreover, the formation of hydrogen bridges between the phosphonate groups P–O–H···O^-–P or with water participation P–O–H···O(H)–H···O^-–P can lead to agglutination of micelles, providing slightly larger charge-stabilized particles. This conclusion is supported by the fact that the cationic analogue of CX8 of very similar architecture, which cannot form this kind of hydrogen bonds yields micelles of small diameter (6.3 nm), which corresponds well to the double length of the molecule [23]. On the other hand, the different orientation of the C780 bis-phosphonic groups presumably favors the formation of intramolecular hydrogen bonds (accordingly to the PM3 calculation) but less intermolecular H-bonds which can only form with two neighboring side-located molecules. As intermolecular interactions are spatially restricted and their number is limited to two per molecule, agglutination of micelles is not favored and, thus, only individual micelles are observed. Interestingly, in 0.15 M NaOH solution, the diameter of CAX8 particles was 8-9 nm, close to the theoretical value (Fig. S5). A higher pH likely deprotonates the phosphonate groups of CAX8, which increases the size of its polar head groups and at the same time prevents their H-bonding, promoting the formation of small micelles. CAX8 and C780 anionic micelles are expected to favor the formation of well-defined complexes with cationic peptides, similar to those observed for cationic micelles and DNA [23].

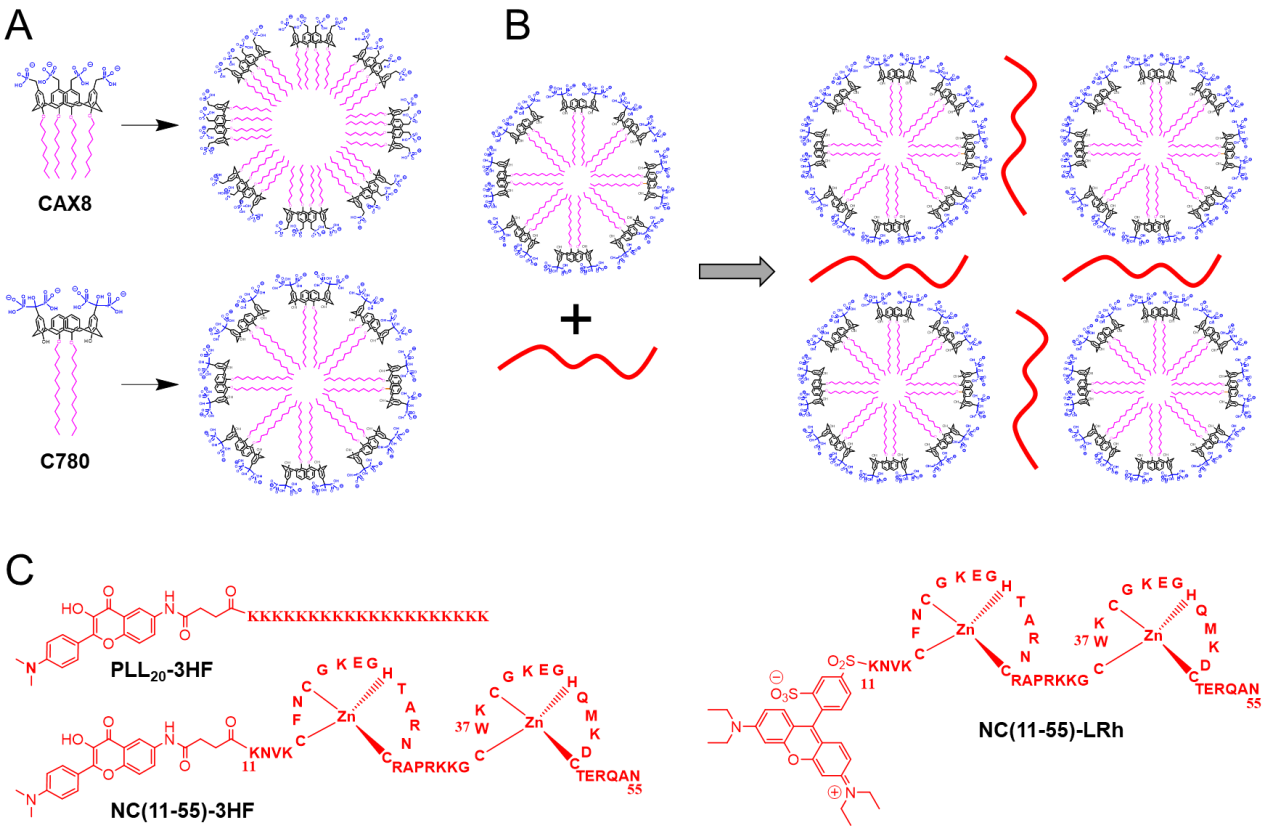

Scheme 2. Schematic presentation of self-assembly of calixarenes in solution without (A) and with (B) cationic peptides (in red). (C) Chemical structures of the fluorescently labelled cationic peptides used in this work.

Interaction with cationic peptides

First, we studied the interaction of calixarene micelles with the model cationic peptide, PLL_{20}-3HF, composed of 20 lysine residues and labelled at its N-terminus with an environmentally sensitive dye, 3-hydroxyflavone (3HF). 3HF dyes exhibit two-band emission spectra attributed to the presence of both its charge transferred normal (N*) state and their tautomer (T*) state, a product of excited-state intramolecular proton transfer (ESIPT) [45]. The N* state shows typical solvent dependent red shifts with an increase in solvent polarity, whereas the T* state appears in less polar environments [46]. This environment sensitivity made 3HF dyes suitable for probing the interaction of peptides within different partners [47], including proteins [48], nucleic acids [49], and lipid membranes [50]. In our titration experiments, the concentration of the labelled peptide (PLL_{20}-3HF) was kept constant, while the calixarene concentration was varied. The formulated calixarene/peptide mixtures had defined molar ratios of the negatively charged phosphonates of calixarene to the positively charged ammonium groups, named as P/N ratio. An increase in CAX8 and C780 concentration (i.e. an increase in the P/N ratio) resulted in an increase of the fluorescence intensity of the label, accompanied by a blue shift in the short-wavelength emission band assigned to the charge-transferred N* state (Figure 2A and B). This blue shift

and intensity increase suggest that the 3HF label senses a decrease in the environment polarity, as a result of the interaction with the amphiphilic calixarenes. Indeed, the alkyl chains in calixarenes lead to micelles with hydrophobic domains which are detected by the 3HF label in the complexes with the peptides. Moreover, in case of C780, a shoulder around 560 nm was observed in the complex (Figure 2B), which can be assigned to a contribution from the T* form (ESIPT product). This indicates an even less polar environment in the peptide complexed with C780 micelles, compared to that of CAX8, which is also in line with its more blue-shifted N* band (511 nm for C780 vs 526 nm for CAX8).

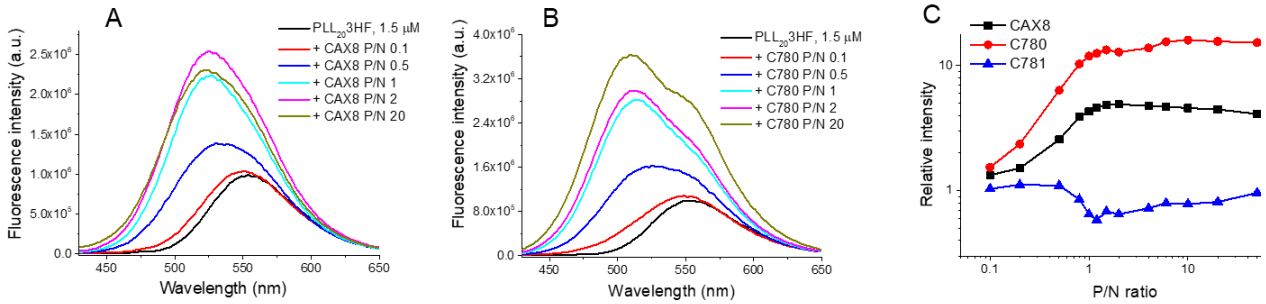

Figure 2. (A, B) Fluorescence spectra of PLL_{20}-3HF in the presence of CAX8 (A) and C780 (B) in 20 mM Tris buffer, pH 7.4 (C) Fluorescence intensity of PLL_{20}-3HF at the maximum (523 nm for CAX8, 509 nm for C780 and 525 nm for C781) in the presence of increasing concentrations of anionic calixarenes divided by the intensity of the PLL_{20}-3HF alone.

The stoichiometry of interaction was determined by plotting the 3HF fluorescence intensity vs the P/N ratio. The major changes in intensity were observed up to a P/N ratio of 1, while above this ratio the intensity changes were minor (Figure 2C). Our data clearly show that the electrostatic interactions of the negatively charged phosphonates of calixarenes with the positively charged ammonium groups of the peptide lead to complexes with calixarene micelles containing hydrophobic domains, probably formed by alkyl chains. In the case of C781, which has short alkyl chains, a blue shift was also observed (Figure S7), but it was smaller, whereas the fluorescence intensity decreased with increasing P/N between 0 and 1 (Figure 2C). This indicates that calixarene C781, unable to form micelles, interacts differently with the peptide.

Table 2. DLS data for PLLs, NC(11-55), and calixarene-polypeptides aggregates.[a]

	PLL4-15				PLL15-30				NC(11-55)			
	P/N=2		P/N=5		P/N=2		P/N=5		P/N=2		P/N=5	
	D, nm	PDI	D, nm	PDI	D, nm	PDI	D, nm	PDI	D, nm	PDI	D, nm	PDI
C780	79.4 ±10.4	0.28 ±0.06	73.5 ±16.3	0.25 ±0.02	88.4 ±11.0	0.18 ±0.03	25.8 ±5.2	0.42 ±0.10	154 ±3	0.13 ±0.02	29.0 ±6.4	0.33 ±0.05
CAX8	194 ±45	0.22 ±0.03	80.7 ±14.9	0.27 ±0.04	112.6 ±4.2	0.22 ±0.03	37.0 ±6.2	0.41 ±0.10	22.0 ±0.6	0.34 ±0.07	18.5 ±0.7	0.36 ±0.04

[a] D is the hydrodynamic diameter; PDI is the polydispersity index. The values are average of 3 measurements; the error is standard deviation.

Next, we studied the size of the obtained complexes using DLS. In this case, we used polylysine (PLL) with a molecular weight of 4000-15000 (PLL4-15) and 15000-30000 (PLL15-30). While PLL alone did not provide consistent DLS data, showing large size and polydispersity, small particles were formed in the presence of calixarenes CAX8 and C780. For both of them, the size of the particles was lower at a higher P/N ratio, reaching 25 nm for C780 with PLL15-30 at P/N = 5 (Table 2). The effect of the P/N ratio was expected as an increasing number of calixarenes in the complexes should increase their net negative charge, favoring stronger repulsion and thus, the formation of smaller particles. This effect is similar to that typically seen with nucleic acids, where the larger access of the positively charged transfection agent results in smaller DNA complexes [51]. In case of complexation of oppositely charged polyelectrolytes, the small-sized nanoparticles are also obtained only when cationic or anionic polymer is present in the excess to ensure strong surface charge required for particle-particle repulsion [52]. Moreover, the larger cationic peptide PLL15-30 provided systematically smaller particles, probably because they ensure stronger complexation with calixarenes. Remarkably, the short-chain calixarene C781 formed with PLL polydisperse unstable particles with a tendency to sediment. This suggests that long hydrophobic chains and the micelle formation are important for obtaining small-sized complexes of calixarenes with peptides. This conclusion is similar to that we previously made for the complexes of the cationic calixarene CX8 with DNA [23].

In the next step, we used NC(11-55), a peptide fragment of the nucleocapsid protein of the human immunodeficiency virus type 1 (HIV-1) that plays multiple functions in the viral cycle [53, 54]. NC(11-55) coordinates two zinc ions and bears 12 basic amino acids (total charge 12+). Similar to PLL, it was labelled with a 3HF label, sensitive to environmental changes. Titration of this labelled peptide with increasing concentrations of calixarenes resulted in a similar fluorescence response of the probe, with a shift to the blue of its emission maximum with increasing P/N ratios (Figure 3). However, the intensity increase was less pronounced than with PLL and an intensity decrease was even observed at low P/N

ratios probably because of aggregation/precipitation of the complexes. Moreover, gradual spectral changes were observed with P/N ratios increasing from 0 to 10 (Figure 3C), which showed that more calixarene molecules were needed to complex this less charged and probably less affine peptide. Calixarene C781 again showed a different behavior (Figure S7) with a significant drop in 3HF fluorescence intensity for most P/N ratios (Figure 3). Overall, the spectral changes with C781 were smaller compared to CAX8 and C780 (Table 3), confirming that C781 is a less attractive peptide complexing agent. For the three calixarenes, the spectral changes were smaller for NC(11-55) than for PLL (Table 3), probably because the former is less charged.

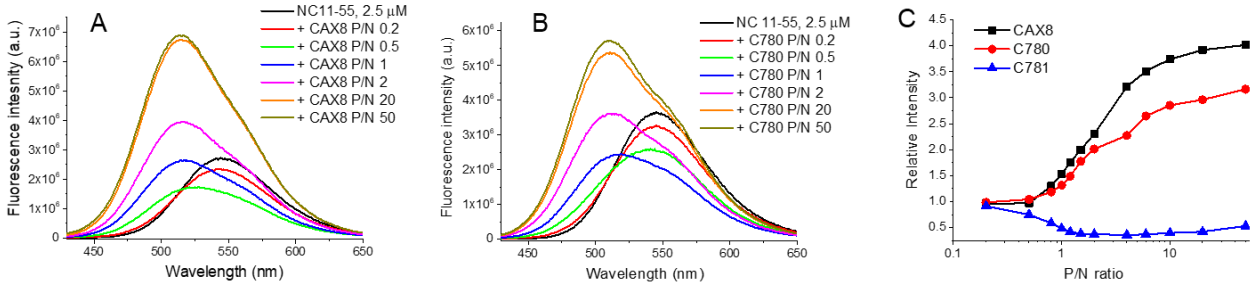

Figure 3. Fluorescence spectra of NC(11-55)-3HF (2.5 µM) in the presence of CAX8 (A) and C780 (B) in 20 mM Tris buffer, pH 7.4. (C) Fluorescence intensity of NC(11-55)-3HF at the maximum (516 nm for CAX8, 511 nm for C780, and 521 nm for C781) in the presence of anionic calixarenes.

Table 3. Fluorescence spectroscopic changes of 3HF-labelled peptides upon interaction with calixarenes.

	CAX8		C780		C781	
	Δ, nm of maximum	Max change of intensity, %	Δ, nm of maximum	Max change of intensity, %	Δ, nm of maximum	Max change of intensity, %
PLL-3HF	-31	+390	-41	+1410	-27	-42
NC(11-55)-3HF	-31	+360	-34	+220	-26	-63

According to DLS, the size of the complexes of NC(11-55) peptide with calixarenes C780 and CAX8 was relatively small and decreased at a higher P/N ratio. The complexes with CAX8 were particularly small, reaching 18.5 nm at P/N = 5 (Table 2). We also verified the size of the complexes using fluorescence correlation spectroscopy, a powerful technique for determining the size of fluorescent nano-objects [55, 56]. The hydrodynamic diameter measured for NC(11-55) labelled with lissamine rhodamine dye (NC(11-55)-LRh, Scheme 2) upon addition of calixarenes increased from 2.2 nm to 10-24 nm (Table

S2). The diameters of the complexes measured by FCS were comparable to those obtained by DLS, confirming that the obtained complexes contained the NC(11-55) peptide (Table S2).

Next, we evaluated cytotoxicity of anionic calixarenes in HeLa cells using commercial CellTiterGlo assay. We found that in the broad range of tested concentrations up to 10 μM, no signs of cytotoxicity were observed, in contrast to a control compound cisplatin. The absence of cytotoxicity, especially for the key compounds CAX8 and C780 is important for their further applications as a vector for peptide delivery.

Finally, we studied the capacity of CAX8 and C780 to promote delivery of a model cationic peptide into the cells. To this end, we studied the internalization of the nanoscale complexes of anionic calixarenes with lissamine rhodamine-labelled NC(11-55) into HeLa cells (Figure 4). Incubation of cells with the free peptide did not reveal any significant internalization of the peptide (Figure 4A,B). In contrast, a clear internalization of the complexes of NC(11-55) with C780 was observed after 3h incubation (Figure 4D), indicating that complexation with anionic calixarenes promoted the internalization of the peptide into the cells. Similar results were observed with CAX8, though some aggregation was observed for the longer (3h) incubation time (Figure 4F). Observation of fluorescent dots is an indication of the endocytic localization of the complexes, which is a typical behavior for nanoparticle formulations [57]. We can thus conclude that the formation of nanoparticles with calixarenes favors the internalization of the peptide by endocytosis.

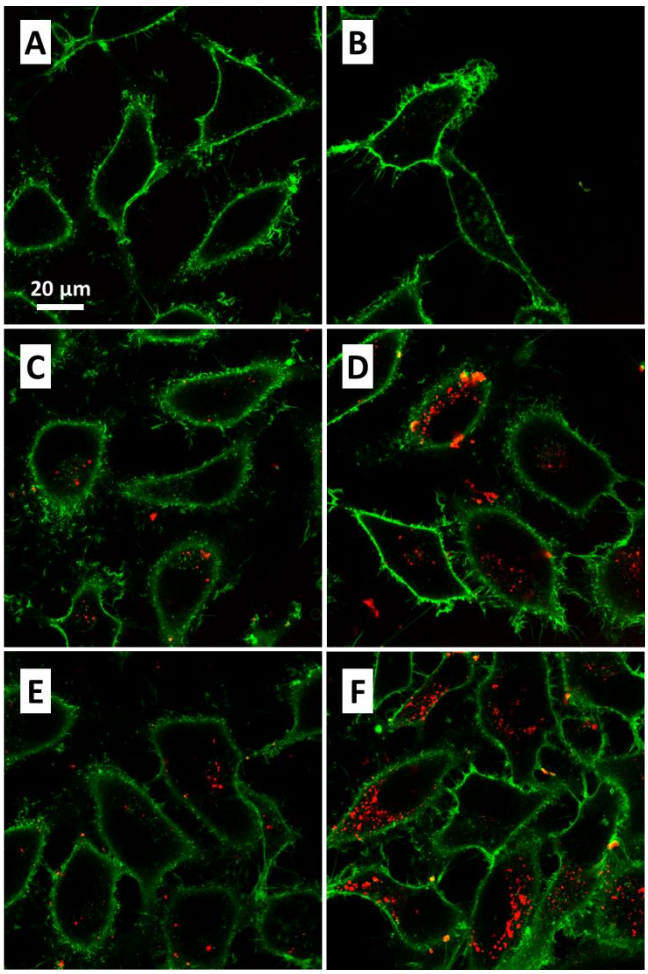

Figure 4. Fluorescence microscopy images of HeLa cells in the presence of free NC(11-55) labeled with lissamine rhodamine dye (NC(11-55)-LRh) (A, B) and its complexes with calixarenes CAX8 (C, D) and C780 (E, F). Incubation times at 37 °C were 1 h (A, C, E) and 3 h (B, D, F). The complexes appear as red dots. Cells were stained in green by a membrane marker WGA-Alexa Fluor488.

Experimental part

Synthesis: All chemicals for synthesis were purchased from Marchrochem or Sigma-Aldrich and they were of Reagent Grade. All reactions were carried out in anhydrous solvents (from Marchrochem or Sigma-Aldrich) under an inert atmosphere. DMF was freshly distilled. THF was dried over K/Na alloy and toluene was distilled over P_2O_5 and then kept with sodium wire. ^{1}H NMR (299.94 MHz) spectra were recorded on a spectrometer "Varian VXR-300" using hexamethyldisiloxane as internal standards. Chemical shifts are given in δ scales (^{1}H). Mass spectra were recorded using Mass Spectrometer Mariner System 5155. Synthesis of peptide NC(11-55) labelled with the MFL probe (NC(11-55)-3HF), a functionalized derivative of 4'-(dimethylamino)-3-hydroxyflavone [50], was described elsewhere [58]. PLL_{20}-3HF was synthesised using the same protocol as for (NC(11-55)-3HF). NC(11-55) labelled at the

N-terminus with lyssamine rhodamine (NC(11-55)-LRh) was synthesised as described elsewhere [58]. All obtained peptides were purified by reverse-phase (C18) HPLC.

General procedure for calixarene acyl chloride 2a,b Thionyl chloride (0.3 mmol) was added to calixarene carboxylic acids **1a,b** (synthesized according to a method described elsewhere [59]) in toluene (20 ml) under argon. One drop of DMF was added to the reaction mixture as a catalyst. The resulting reaction mixture was heated to 100 ^{o}C for 2 hours. The solvents were distilled off under reduced pressure and the residue was washed with hexane to afford a colourless solid. Thus obtained acyl chlorides 5,17-dicarbochlorid-26,28- didodecyloxy-25,27-dihydroxycalix[4]arene (**2a**) and 5,17-dicarbochlorid-26,28-dipropoxy-25,27-dihydroxycalix[4]arene (**2b**) were used in the next step without further purifications.

General procedure for the preparation of calixarene hydroxybisphosphonous acids C780 and C781

To a solution of calixarene acyl chloride **2a,b** (0.1 mmol) in 20 mL dry THF tris(trimethylsilyl)phosphite (8 mmol) was added under argon. The reaction mixture was then stirred at 35 ^{o}C for 8 h. After evaporation of volatile fractions under reduced pressure, the crude product was hydrolyzed with wet methanol for 2 h at room temperature. After evaporation of the solvent under vacuum, the obtained compound was washed with diethyl ether. Yields 90-96 %.

5,17-Bis-(1-hydroxymethyl-1,1-bis(dihydroxyphosphoryl)-25,27-didodecyloxycalix[4]arene (**C780**). White solid: yield 90%; m.p. 124-126 ^{o}C; ^{1}H NMR (DMSO-d_6) δ: 8.3 (wide s, 2H, PhO*H*); 7.58 (wide s, 4H, Ar*H*); 7.19 (wide s, 4H, Ar*H*); 6.71 (wide s, 2H, Ar*H*); 4.25 (d, 4H, J 13.2 Hz**,** ArCH_{2ax}); 4.05 (t, 4H, J 7.5 Hz, OCH_2), 3.32 (d, 4H, J 13.2 Hz**,** ArCH_{2eq}), 1.96 (m, 4H $CH_3CH_2CH_2O$), 1.29 (m, 36H, $CH_3(CH_2)_9CH_2CH_2O$), 0.85 (t, 6H, J 7.5 Hz, $O(CH_2)_{11}CH_3$), ^{31}P NMR δ 19.1. MS (FAB) *m/z*; 1142.0 $[M+H]^+$. Calculated: 1142.1.

5,17-Bis-(1-hydroxymethyl-1,1-bis(dihydroxyphosphoryl)-25,27-dipropoxycalix[4]arene (**C781**). White solid: yield 96%; m.p. 187-189 ^{o}C; ^{1}H NMR (DMSO-d_6) δ: 8.4 (wide s, 2H, PhO*H*); 7.63 (wide s, 4H, Ar*H*); 7.23 (wide s, 4H, Ar*H*); 6.79 (wide s, 2H, Ar*H*); 4.23 (d, 4H, J 13.2 Hz**,** ArCH_{2ax}); 3.98 (t, 4H, J 7.5 Hz, OC$H_2CH_2CH_3$), 3.36 (d, 4H, J 13.2 Hz**,** ArCH_{2eq}), 2.05 (m, $CH_3CH_2CH_2O$), 1.24 (t, 6H, J 7.5 Hz, CH_2CH_3), ^{31}P NMR δ 19.6. MS (FAB) *m/z*; 890.0 $[M+H]^+$. Calculated: 889.6.

5,11,17,23-tetrakis(dihydroxyphosphonylmethyl)-25,26,27,28- tetraoctyloxycalix[4]arene (**CAX8**).

To calixarene **3** (0.1 mmol), tris(trimethylsilyl)phosphite (20 mmol) was added under argon. The reaction mixture was then stirred at 100 ^{o}C for 3 h. After evaporation of volatile fractions under reduced pressure, the crude product was hydrolyzed with wet methanol for 2 h at room temperature. After evaporation of the solvent under vacuum, the obtained compound was washed with diethyl ether. White solid: yield 95%; m.p. 95-97 ^{o}C; ^{1}H NMR (DMSO-d_6+5% CF_3COOD) 6.59 (wide s, 4H, Ar*H*); 4.24 (d, 4H, J 13.2 Hz**,** ArCH_{2ax}); 3.73 (t, 8H, J 7.5 Hz, OCH_2), 3.30 (d, 4H, J 13.2 Hz**,** ArCH_{2eq}), 2.72 (d, 8H, J

15.9 Hz**,** $ArCH_2$),1.86 (m, 40H, $CH_3(CH_2)_5CH_2CH_2O$), 0.85 (t, 6H, J 7.5 Hz, $O(CH_2)_7CH_3$), ^{31}P NMR δ 18.5. MS (FAB) *m/z*; 1250.4 $[M+H]^+$. Calculated: 1250.3.

Dynamic light scattering and zeta potential measurements: The complexes of calixarenes with PLL4000-15000 and PLL15000-30000 (Sigma-Aldrich) or NC(11-55) in a form of a zinc complex (synthesized as described previously [49]) were prepared by mixing equal volumes of PLL or NC(11-55) and calixarene in 20 mM Tris (pH 7.4) buffer. The final PLL (by lysine moieties) concentration was 20 μM, the final NC(11-55) (by basic amino acids) concentration was 20 μM, while the calixarene concentration was varied to provide the final P/N. The P/N ratio between calixarene and peptide was expressed as the molar ratio between all the dihydroxyphosphoryl groups of the calixarene and the lysine or lysine+arginine groups of the peptide. DLS measurements were done after 30 min of incubation at room temperature. The average size of the complexes was determined with a Zetasizer ZSP (Malvern Instruments) using statistics by volume.

Fluorescence measurements: Absorption spectra were recorded on a Cary 4000 spectrophotometer (Varian) and fluorescence spectra on a FluoroMax 3.0 or Fluorolog (Jobin Yvon, Horiba) spectrofluorometer. All the spectra were corrected for the fluorescence of the blank (corresponding solution without the fluorescence dye). For CMC measurements with pyrene, a 20 mM Tris buffer (pH 7.4) solution, containing 0.6 μM pyrene was titrated with increasing quantities of calixarenes, added from the stock solution in water. For peptide binding experiments PLL_{20}-3HF 1.5 μM (corresponded to 30 μM of basic amino acids) or NC(11-55)-3HF 2.5 μM (corresponded to 30 μM of basic amino acids concentration) in 20 mM Tris buffer (pH 7.4) were prepared. Fluorescence intensity at 506-525 nm, excited at 410 nm, was recorded 1 min after each calixarene addition and then plotted as a function of the corresponding P/N ratio.

FCS setup and data analysis: FCS measurements were performed on a two-photon platform including an Olympus IX70 inverted microscope, as described previously [56]. Two-photon excitation at 850 nm is provided by a mode-locked Tsunami Ti:sapphire laser pumped by a Millenia V solid state laser (Spectra Physics). The measurements were carried out in an eight-well Lab-Tek II coverglass system, using a 300 μL volume per well. The focal spot was set about 20 μm above the coverslip. The normalized autocorrelation function, $G(\tau)$ was calculated online by an ALV-5000E correlator (ALV, Germany) from the fluorescence fluctuations, $\delta F(t)$, by $G(\tau)=\langle \delta F(t)\delta F(t+\tau)\rangle / \langle F(t)\rangle^2$ where $\langle F(t)\rangle$ is the mean fluorescence signal, and τ is the lag time. Assuming that emissive species undergo triplet blinking and diffuse freely in a Gaussian excitation volume, the correlation function, $G(\tau)$, calculated from the fluorescence fluctuations was fitted according to the following equation:

$$G(\tau) = \frac{1}{N}\left(1+\frac{\tau}{\tau_d}\right)^{-1}\left(1+\frac{1}{S^2}\frac{\tau}{\tau_d}\right)^{-1/2}\left(1+\left(\frac{f_t}{1-f_t}\right)\exp\left(-\tau/\tau_t\right)\right)$$

where τ_d is the diffusion time, N is the mean number of molecules within the sample volume, S is the ratio between the axial and lateral radii of the sample volume, f_t is the mean fraction of fluorophores in their triplet state and τ_t is the triplet state lifetime. The excitation volume is about 0.34 fL and S is about 3 to 4. Typical data recording times were 10 min. The final NC(11-55) concentration was 1.7 μM (20 μM by basic amino acids), while the calixarene concentration was varied to provide the final P/N. FCS measurements were done after 30 min of incubation at room temperature. Using carboxytetramethylrhodamine (TMR) in water as a reference, the particle hydrodynamic diameter ($d_{particle}$) was calculated by: $d_{particle} = d_{TMR} \times \tau_{d(particle)}/\tau_{d(TMR)}$ where $\tau_{d(TMR)}$ and $\tau_{d(particle)}$ were the measured correlation times for TMR and our particles, respectively, while d_{TMR}, the hydrodynamic diameter of TMR, was assumed to be 1 nm.

Cytotoxicity evaluation: HeLa cells (ATCC CCL-2) were seeded on the assay plate at concentration 3.3×10^3 cells/well (30 uL/well) and incubated for 24 h at 37ºC, 5% CO2. DMEM with 10% FBS, 1 mM sodium pyruvate, 1% pen/strep was used a growth medium. The following day, test compounds were diluted in growth medium to obtain 8 concentration points (in 6 repetitions) and added to cells (15 ul/well) for 72 h incubation at 37ºC, 5% CO2. The cell viability was determined with CellTiterGlo (Promega) reagent following manufacturer protocol using BMG Pherastar plate reader.

Cellular imaging studies: HeLa cells (ATCC CCL-2) were grown in DMEM (Gibco–Invitrogen), supplemented with 10% fetal bovine serum (Dominique Dutscher) and 1% antibiotic solution (penicillin-streptomycin, Lonza) at 37 °C in a humidified atmosphere containing 5% CO_2. Cells were seeded onto an 8-chambered LabTek slide at a density of 2×10^4 cells per well 24 h before the microscopy measurement. Then, labelled peptide NC(11-55)-LRh (0.125 μM, 1.5 μM by basic amino acids) and its complexes with calixarenes CAX8 and C780 (P/N = 5) were incubated with cells in OptiMEM for 1 and 3 h. Cell membrane staining with wheat-germ agglutinin-Alexa488 (WGA-Alexa488) was done for 5 min at room temperature before the measurements. Fluorescence imaging of the cells was performed using a Leica TSC SPE confocal microscope equipped with a 63× oil immersion objective. The following channels were used: excitation 488 nm, emission recorded from 495 to 560 nm for WGA-Alexa488; excitation 561 nm, emission recorded from 570 to 610 nm for NC(11-55)-LRh and its complexes with calixarenes.

Conclusions

Understanding the design principles and assembly of anionic macrocycles is a path towards development of functional nanocarriers for delivery of biomolecules in biological applications. In the present work,

we hypothesized that anionic amphiphilic calixarenes of conic shape can assemble into negatively charged micellar nanostructures capable to complex cationic peptides into nanoparticles for their delivery into live cells. We designed and synthesized two new amphiphilic calixarenes, both bearing four phosphonate groups, with two or four long alkyl chains. Fluorescence studies using pyrene probe suggested that both calixarenes form micelles in the micromolar concentration range. In contrast, a calixarene bearing two short alkyl chains showed no signs of micelle formation. According to dynamic light scattering, a calixarene with perfect conical shape (bearing two long alkyl chains) form micelles of ~10 nm diameter. In the case of the calixarene with four alkyl chains, 10 nm micelles were obtained only at high pH. This high pH is required to ensure proper hydrophilic/hydrophobic balance and prevent intermolecular H-bonding, in order to inhibit aggregation of calixarenes into larger particles. These results provide new insights on the rational design of anionic macrocycles for their further assembly into small micellar structures. So far, this was mainly established for cationic amphiphilic calixarenes [23, 34, 60]. Complexation of the anionic calixarenes with cationic peptides, such as 20-mer polylysine and the biologically relevant HIV-1 nucleocapsid peptide, was further studied. Using an environment-sensitive label of the 3-hydroxyflavone family grafted to these peptides, we observed the formation of calixarene/peptide complexes with well-defined stoichiometry: at the anion (phosphonate) to cation (ammonium) ratio close to 1, revealing the importance of electrostatic interactions. Dynamic light scattering and fluorescence correlation spectroscopy indicated the formation of small nanoparticles (20-40 nm) with both amphiphilic calixarenes. In contrast, an anionic calixarene with short alkyl chains yielded large polydisperse particles, highlighting the importance of hydrophobic interactions and micellar assembly of amphiphilic calixarenes for peptide complexation. Thus, we provide the first evidence that anionic amphiphilic macrocycles, preassembled into micelles, are capable to complex cationic peptides into small nanoparticles. Previously, this was shown for cationic and glycosylated amphiphilic macrocycles for complexation of anionic biomolecules (nucleic acids) [16, 22, 23, 26, 32-34, 43]. The anionic calixarenes showed negligible cytotoxicity in the tested concentration range (up to 10 μM), indicating that these molecules could be applied in biological studies. We could speculate that shape-persistent conic nature of these anionic calixarenes makes them particularly prone to self-assembly into micelles, rather than to interact and destabilize cell membranes. Cellular studies using fluorescence microscopy with a model labelled peptide revealed that that the amphiphilic calixarenes drastically enhance the internalization of the peptides into live cells, likely through endocytosis. We expect that formation of complexes with calixarenes favors interaction of the peptide with cells, which helps its further internalization. More work on the design of amphiphilic calixarenes will be needed to further achieve delivery of the peptide into cytosol of the cells [14, 61]. For example, the use of groups that could be protonated at low pH (e.g. imidazole, etc) could induce a “proton sponge” effect, leading to the

endosomal escape [62-65]. The obtained results suggest anionic amphiphilic macrocycles as promising peptide delivery vehicles.

Acknowledgement

This work was supported by PICS program 6053 (CNRS of France and NAS of Ukraine) and European Research Council ERC Consolidator grant BrightSens 648528. R.V.R., S.O.C., and V.I.K. thank National Research Fund of Ukraine for partial support of their work through grant 2020.02/0031. Y.M. is grateful to the "Institut Universitaire de France (IUF)" for support and providing additional time to be dedicated to research.

CRediT author statement

Roman V. Rodik: Conceptualization, Methodology, Investigation, Data Curation, Writing - Original Draft, Writing - Review & Editing, Visualization. **Sergiy O. Cherenok:** Methodology, Investigation. **Viktoriia Y. Postupalenko:** Methodology, Investigation. **Sule Oncul:** Methodology, Investigation. **Vladyslava Brusianska:** Methodology, Investigation. **Petro Borysko:** Methodology, Investigation. **Vitaly I. Kalchenko:** Conceptualization, Project administration, Funding acquisition. **Yves Mely:** Methodology, Project administration. **Andrey S. Klymchenko:** Conceptualization, Methodology, Investigation, Writing - Original Draft, Writing - Review & Editing, Visualization, Supervision, Project administration, Funding acquisition.

References

[1] R.E.W. Hancock, H.G. Sahl, Antimicrobial and host-defense peptides as new anti-infective therapeutic strategies, Nat. Biotechnol. 24 (2006) 1551-1557.
[2] P. Vlieghe, V. Lisowski, J. Martinez, M. Khrestchatisky, Synthetic therapeutic peptides: science and market, Drug Discov. Today 15 (2010) 40-56.
[3] J.L. Lau, M.K. Dunn, Therapeutic peptides: Historical perspectives, current development trends, and future directions, Bioorg. Med. Chem. 26 (2018) 2700-2707.
[4] A.W. Du, M.H. Stenzel, Drug Carriers for the Delivery of Therapeutic Peptides, Biomacromolecules 15 (2014) 1097-1114.
[5] V.P. Torchilin, A.N. Lukyanov, Peptide and protein drug delivery to and into tumors: challenges and solutions, Drug Discov. Today 8 (2003) 259-266.
[6] R. Nordstrom, M. Malmsten, Delivery systems for antimicrobial peptides, Adv. Colloid Interface Sci. 242 (2017) 17-34.
[7] M. Mae, U. Langel, Cell-penetrating peptides as vectors for peptide, protein and oligonucleotide delivery, Curr. Opin. Pharmacol. 6 (2006) 509-514.
[8] F. Heitz, M.C. Morris, G. Divita, Twenty years of cell-penetrating peptides: from molecular mechanisms to therapeutics, Br. J. Pharmacol. 157 (2009) 195-206.
[9] M. Akishiba, T. Takeuchi, Y. Kawaguchi, K. Sakamoto, H.H. Yu, I. Nakase, T. Takatani-Nakase, F. Madani, A. Graslund, S. Futaki, Cytosolic antibody delivery by lipid-sensitive endosomolytic peptide, Nat. Chem. 9 (2017) 751-761.

[10] K. Braun, A. Pochert, M. Linden, M. Davoudi, A. Schmidtchen, R. Nordstrom, M. Malmsten, Membrane interactions of mesoporous silica nanoparticles as carriers of antimicrobial peptides, J. Colloid Interface Sci. 475 (2016) 161-170.
[11] D.J. McClements, Encapsulation, protection, and delivery of bioactive proteins and peptides using nanoparticle and microparticle systems: A review, Adv. Colloid Interface Sci. 253 (2018) 1-22.
[12] M. Gontsarik, A. Ben Mansour, L.D. Hong, M. Guizar-Sicairos, S. Salentinig, pH-responsive aminolipid nanocarriers for antimicrobial peptide delivery, J. Colloid Interface Sci. 603 (2021) 398-407.
[13] Y.-W. Lee, D.C. Luther, R. Goswami, T. Jeon, V. Clark, J. Elia, S. Gopalakrishnan, V.M. Rotello, Direct Cytosolic Delivery of Proteins through Coengineering of Proteins and Polymeric Delivery Vehicles, J. Am. Chem. Soc. 142 (2020) 4349-4355.
[14] V. Postupalenko, A.P. Sibler, D. Desplancq, Y. Nomine, D. Spehner, P. Schultz, E. Weiss, G. Zuber, Intracellular delivery of functionally active proteins using self-assembling pyridylthiourea-polyethylenimine, J. Control. Release 178 (2014) 86-94.
[15] G. Gasparini, E.-K. Bang, J. Montenegro, S. Matile, Cellular uptake: lessons from supramolecular organic chemistry, Chem. Commun. 51 (2015) 10389-10402.
[16] R.V. Rodik, A.S. Klymchenko, Y. Mely, V.I. Kalchenko, Calixarenes and related macrocycles as gene delivery vehicles, J. Incl. Phenom. Macrocycl. Chem. 80 (2014) 189-200.
[17] S. Walker, R. Oun, F.J. McInnes, N.J. Wheate, The Potential of Cucurbit n urils in Drug Delivery, Isr. J. Chem. 51 (2011) 616-624.
[18] K.C. Jie, Y.J. Zhou, Y. Yao, F.H. Huang, Macrocyclic amphiphiles, Chem. Soc. Rev. 44 (2015) 3568-3587.
[19] H.Z. Bai, J.W. Wang, Z.B. Li, G.P. Tang, Macrocyclic Compounds for Drug and Gene Delivery in Immune-Modulating Therapy, Int. J. Mol. Sci. 20 (2019) 15.
[20] I. Shulov, R.V. Rodik, Y. Arntz, A. Reisch, V.I. Kalchenko, A.S. Klymchenko, Protein-Sized Bright Fluorogenic Nanoparticles Based on Cross-Linked Calixarene Micelles with Cyanine Corona, Angew. Chem. Int. Ed. Engl. 55 (2016) 15884-15888.
[21] J. Murray, K. Kim, T. Ogoshi, W. Yao, B.C. Gibb, The aqueous supramolecular chemistry of cucurbit n urils, pillar n arenes and deep-cavity cavitands, Chem. Soc. Rev. 46 (2017) 2479-2496.
[22] Y. Aoyama, Macrocyclic glycoclusters: From amphiphiles through nanoparticles to glycoviruses, Chem. Eur. J. 10 (2004) 588-593.
[23] R.V. Rodik, A.S. Klymchenko, N. Jain, S.I. Miroshnichenko, L. Richert, V.I. Kalchenko, Y. Mely, Virus-Sized DNA Nanoparticles for Gene Delivery Based on Micelles of Cationic Calixarenes, Chem. Eur. J. 17 (2011) 5526-5538.
[24] L. Baldini, A. Casnati, F. Sansone, Multivalent and Multifunctional Calixarenes in Bionanotechnology, European J. Org. Chem. 2020 (2020) 5056-5069.
[25] R. Kumar, A. Sharma, H. Singh, P. Suating, H.S. Kim, K. Sunwoo, I. Shim, B.C. Gibb, J.S. Kim, Revisiting Fluorescent Calixarenes: From Molecular Sensors to Smart Materials, Chem. Rev. 119 (2019) 9657-9721.
[26] Y. Aoyama, T. Kanamori, T. Nakai, T. Sasaki, S. Horiuchi, S. Sando, T. Niidome, Artificial viruses and their application to gene delivery. size-controlled gene coating with glycocluster nanoparticles, J. Am. Chem. Soc. 125 (2003) 3455-3457.
[27] C. Sathiyajith, R.R. Shaikh, Q. Han, Y. Zhang, K. Meguellati, Y.W. Yang, Biological and related applications of pillar n arenes, Chem. Commun. 53 (2017) 677-696.
[28] X. Wu, L. Gao, X.Y. Hu, L.Y. Wang, Supramolecular Drug Delivery Systems Based on Water-Soluble Pillar n arenes, Chem. Rec. 16 (2016) 1216-1227.
[29] I. Nierengarten, M. Nothisen, D. Sigwalt, T. Biellmann, M. Holler, J.S. Remy, J.F. Nierengarten, Polycationic Pillar 5 arene Derivatives: Interaction with DNA and Biological Applications, Chem. Eur. J. 19 (2013) 17552-17558.
[30] S.J. Barrow, S. Kasera, M.J. Rowland, J. del Barrio, O.A. Scherman, Cucurbituril-Based Molecular Recognition, Chem. Rev. 115 (2015) 12320-12406.
[31] H. Chen, Y.Y. Chen, H. Wu, J.F. Xu, Z.W. Sun, X. Zhang, Supramolecular polymeric chemotherapy based on cucurbit 7 uril-PEG copolymer, Biomaterials 178 (2018) 697-705.

[32] F. Sansone, M. Dudic, G. Donofrio, C. Rivetti, L. Baldini, A. Casnati, S. Cellai, R. Ungaro, DNA condensation and cell transfection properties of guanidinium calixarenes: Dependence on macrocycle lipophilicity, size, and conformation, J. Am. Chem. Soc. 128 (2006) 14528-14536.
[33] V. Bagnacani, V. Franceschi, M. Bassi, M. Lomazzi, G. Donofrio, F. Sansone, A. Casnati, R. Ungaro, Arginine clustering on calix 4 arene macrocycles for improved cell penetration and DNA delivery, Nat. Commun. 4 (2013) 7.
[34] R.V. Rodik, A.S. Anthony, V.I. Kalchenko, Y. Mely, A.S. Klymchenko, Cationic amphiphilic calixarenes to compact DNA into small nanoparticles for gene delivery, New J. Chem. 39 (2015) 1654-1664.
[35] C.-X. Yu, F.-L. Hu, J.-G. Song, J.-L. Zhang, S.-S. Liu, B.-X. Wang, H. Meng, L.-L. Liu, L.-F. Ma, Ultrathin two-dimensional metal-organic framework nanosheets decorated with tetra-pyridyl calix[4]arene: Design, synthesis and application in pesticide detection, Sens. Actuators B Chem. 310 (2020) 127819.
[36] Z. Liu, X. Dai, Y. Sun, Y. Liu, Organic supramolecular aggregates based on water-soluble cyclodextrins and calixarenes, Aggregate 1 (2020) 31-44.
[37] C. Chen, X. Ni, H.-W. Tian, Q. Liu, D.-S. Guo, D. Ding, Calixarene-Based Supramolecular AIE Dots with Highly Inhibited Nonradiative Decay and Intersystem Crossing for Ultrasensitive Fluorescence Image-Guided Cancer Surgery, Angew. Chem. Int. Ed. Engl. 59 (2020) 10008-10012.
[38] X. Fan, X. Guo, Development of calixarene-based drug nanocarriers, J. Mol. Liq. 325 (2021) 115246.
[39] Y.-C. Pan, X.-Y. Hu, D.-S. Guo, Biomedical Applications of Calixarenes: State of the Art and Perspectives, Angew. Chem. Int. Ed. Engl. 60 (2021) 2768-2794.
[40] E. Amirthalingam, M. Rodrigues, L. Casal-Dujat, A.C. Calpena, D.B. Amabilino, D. Ramos-Lopez, L. Perez-Garcia, Macrocyclic imidazolium-based amphiphiles for the synthesis of gold nanoparticles and delivery of anionic drugs, J. Colloid Interface Sci. 437 (2015) 132-139.
[41] W.C. Geng, Q.X. Huang, Z. Xu, R.B. Wang, D.S. Guo, Gene delivery based on macrocyclic amphiphiles, Theranostics 9 (2019) 3094-3106.
[42] J.A. Lebron, M. Lopez-Lopez, C.B. Garcia-Calderon, I.V. Rosado, F.R. Balestra, P. Huertas, R.V. Rodik, V.I. Kalchenko, E. Bernal, M.L. Moya, P. Lopez-Cornejo, F.J. Ostos, Multivalent Calixarene-Based Liposomes as Platforms for Gene and Drug Delivery, Pharmaceutics 13 (2021) 26.
[43] J. Gasparello, A. Manicardi, A. Casnati, R. Corradini, R. Gambari, A. Finotti, F. Sansone, Efficient cell penetration and delivery of peptide nucleic acids by an argininocalix 4 arene, Sci. Rep. 9 (2019) 10.
[44] V.V. Trush, S.O. Cherenok, V.Y. Tanchuk, V.P. Kukhar, V.I. Kalchenko, A.I. Vovk, Calix 4 arene methylenebisphosphonic acids as inhibitors of protein tyrosine phosphatase 1B, Bioorg. Med. Chem. Lett. 23 (2013) 5619-5623.
[45] P.K. Sengupta, M. Kasha, Excited-state proton-transfer spectroscopy of 3-hydroxyflavone and quercetin, Chem. Phys. Lett. 68 (1979) 382-385.
[46] A.S. Klymchenko, A.P. Demchenko, Multiparametric probing of intermolecular interactions with fluorescent dye exhibiting excited state intramolecular proton transfer, Phys. Chem. Chem. Phys. 5 (2003) 461-468.
[47] A.S. Klymchenko, Solvatochromic and Fluorogenic Dyes as Environment-Sensitive Probes: Design and Biological Applications, Acc. Chem. Res. 50 (2017) 366-375.
[48] K. Enander, L. Choulier, A.L. Olsson, D.A. Yushchenko, D. Kanmert, A.S. Klymchenko, A.P. Demchenko, Y. Mely, D. Altschuh, A peptide-based, ratiometric biosensor construct for direct fluorescence detection of a protein analyte, Bioconjugate Chem. 19 (2008) 1864-1870.
[49] V.V. Shvadchak, A.S. Klymchenko, H. de Rocquigny, Y. Mely, Sensing peptide-oligonucleotide interactions by a two-color fluorescence label: application to the HIV-1 nucleocapsid protein, Nucleic Acids Res. 37 (2009) 12.
[50] V.Y. Postupalenko, V.V. Shvadchak, G. Duportail, V.G. Pivovarenko, A.S. Klymchenko, Y. Mely, Monitoring membrane binding and insertion of peptides by two-color fluorescent label, Biochim. Biophys. Acta Biomembr. 1808 (2011) 424-432.
[51] M.A. Mintzer, E.E. Simanek, Nonviral Vectors for Gene Delivery, Chem. Rev. 109 (2009) 259-302.

[52] A. Combes, K.-N. Tang, A.S. Klymchenko, A. Reisch, Protein-like particles through nanoprecipitation of mixtures of polymers of opposite charge, J. Colloid Interface Sci. 607 (2022) 1786-1795.
[53] J.L. Darlix, J. Godet, R. Ivanyi-Nagy, P. Fosse, O. Mauffret, Y. Mely, Flexible Nature and Specific Functions of the HIV-1 Nucleocapsid Protein, J. Mol. Biol. 410 (2011) 565-581.
[54] H. Beltz, C. Clauss, E. Piemont, D. Ficheux, R.J. Gorelick, B. Roques, C. Gabus, J.L. Darlix, H. de Rocquigny, Y. Mely, Structural determinants of HIV-1 nucleocapsid protein for cTAR DNA binding and destabilization, and correlation with inhibition of self-primed DNA synthesis, J. Mol. Biol. 348 (2005) 1113-1126.
[55] D. Wöll, Fluorescence correlation spectroscopy in polymer science, RSC Adv. 4 (2014) 2447-2465.
[56] A.S. Klymchenko, E. Roger, N. Anton, H. Anton, I. Shulov, J. Vermot, Y. Mely, T.F. Vandamme, Highly lipophilic fluorescent dyes in nano-emulsions: towards bright non-leaking nano-droplets, RSC Adv. 2 (2012) 11876-11886.
[57] G. Sahay, D.Y. Alakhova, A.V. Kabanov, Endocytosis of nanomedicines, J. Control. Release 145 (2010) 182-195.
[58] N. Kempf, V. Postupalenko, S. Bora, P. Didier, Y. Arntz, H. de Rocquigny, Y. Mely, The HIV-1 Nucleocapsid Protein Recruits Negatively Charged Lipids To Ensure Its Optimal Binding to Lipid Membranes, J. Virol. 89 (2015) 1756-1767.
[59] A. Casnati, M. Fochi, P. Minari, A. Pochini, M. Reggiani, R. Ungaro, D.N. Reinhoudt, Upper-rim urea-derivatized calix 4 arenes as neutral receptors for monocarboxylate anions, Gazz. Chim. Ital. 126 (1996) 99-106.
[60] S. Arimori, T. Nagasaki, S. Shinkai, Self-assembly of tetracationic amphiphiles bearing a calix[4]arene core. Correlation between the core structure and the aggregation properties, J. Chem. Soc., Perkin Trans. 2 2 (1995) 679-683.
[61] V. Postupalenko, D. Desplancq, I. Orlov, Y. Arntz, D. Spehner, Y. Mely, B.P. Klaholz, P. Schultz, E. Weiss, G. Zuber, Protein Delivery System Containing a Nickel-Immobilized Polymer for Multimerization of Affinity-Purified His-Tagged Proteins Enhances Cytosolic Transfer, Angew. Chem. Int. Ed. Engl. 54 (2015) 10583-10586.
[62] P. Midoux, C. Pichon, J.J. Yaouanc, P.A. Jaffres, Chemical vectors for gene delivery: a current review on polymers, peptides and lipids containing histidine or imidazole as nucleic acids carriers, Br. J. Pharmacol. 157 (2009) 166-178.
[63] T.F. Martens, K. Remaut, J. Demeester, S.C. De Smedt, K. Braeckmans, Intracellular delivery of nanomaterials: How to catch endosomal escape in the act, Nano Today 9 (2014) 344-364.
[64] T. Bus, A. Traeger, U.S. Schubert, The great escape: how cationic polyplexes overcome the endosomal barrier, J. Mater. Chem. B 6 (2018) 16.
[65] A. Dhankher, W. Lv, W.T. Studstill, J.A. Champion, Coiled coil exposure and histidine tags drive function of an intracellular protein drug carrier, J. Control. Release 339 (2021) 248-258.